Two-photon-induced singlet fission in rubrene single crystal

Lin Ma,[1] Gegham Galstyan,[2] Keke Zhang,[3] Christian Kloc,[3] Handong Sun,[1] Cesare Soci,[1] Maria E. Michel-Beyerle,[1] and Gagik G. Gurzadyan[1,a)]
[1]*Division of Physics and Applied Physics, School of Physical and Mathematical Sciences, Nanyang Technological University, Singapore 637371, Singapore*
[2]*Department of Biology, Chemistry and Pharmacy, Free University of Berlin, Berlin 14195, Germany*
[3]*Division of Materials Science, School of Materials Science and Engineering, Nanyang Technological University, Singapore 639798, Singapore*

(Received 26 February 2013; accepted 26 April 2013; published online 14 May 2013)

The two-photon-induced singlet fission was observed in rubrene single crystal and studied by use of femtosecond pump-probe spectroscopy. The location of two-photon excited states was obtained from the nondegenerate two-photon absorption (TPA) spectrum. Time evolution of the two-photon-induced transient absorption spectra reveals the direct singlet fission from the two-photon excited states. The TPA absorption coefficient of rubrene single crystal is 52 cm/GW at 740 nm, as obtained from Z-scan measurements. Quantum chemical calculations based on time-dependent density functional theory support our experimental data. © *2013 AIP Publishing LLC*. [http://dx.doi.org/10.1063/1.4804398]

I. INTRODUCTION

Rubrene, a tetraphenyl derivative of tetracene, well known for its high hole mobility,[1,2] was extensively studied in recent years. Different spectroscopic techniques were applied to study the dynamics of photophysical processes in rubrene, like transient absorption (TA) by flash photolysis,[3,4] femtosecond pump-probe technique,[5–7] time resolved photoluminescence,[8] and photon echo.[9] From the studies of the photoexcited state dynamics, singlet fission, from which a singlet excited molecule shares its energy with a neighboring molecule in ground state, and both molecules form a pair of triplet states,[10,11] is proven to take place in the rubrene single crystal.[5–8] Rubrene molecule is centrosymmetric, therefore, the selection rules for one- and two-photon absorption (TPA) are different.[12,13] There are few theoretical[12] and experimental[13] investigations on the nonlinear properties of rubrene. However, the experimental study on two-photon excited state dynamics and the TPA coefficient in both rubrene solution and crystal are still missing.

In this work, to the best of our knowledge for the first time we observed direct singlet fission from two-photon excited upper electronic states in rubrene single crystal. Nondegenerate two-photon absorption (ND-TPA) spectra were obtained under two-photon excitation by use of pump probe technique.[14,15] Compared with linear absorption spectra, the two-photon excited states are located well above the one-photon excited states, which is also supported by quantum chemical calculations. In addition, Z-scan technique was applied in order to measure degenerate TPA coefficient of rubrene crystal.

a)Author to whom correspondence should be addressed. Electronic mail: gurzadyan@ntu.edu.sg

II. METHOD

A. Experimental methods

Rubrene single crystals were grown by physical vapor transport (PVT) technique.[16] The detailed growing procedure is described in Ref. 7. It is notable that only crystals with very thin thickness (less than 10 μm) were chosen for the transient absorption measurements, because rubrene crystal has strong absorption in the visible region (Fig. 1(a)) where there is also the transient absorption signal. In order to detect the transient absorption signal, we need thin crystal sample to keep the transparency in all probing region. For Z-scan measurements, uniform and big size sample (with thickness 20 μm) was chosen to ensure the good quality of transmitted laser beam.

The TA spectra were measured by the optical femtosecond pump probe spectroscopy, the output of titanium-sapphire (Legend Elite, Coherent) regenerative amplifier seeded by the oscillator (Micra, Coherent) was used as a pulsed laser source. The output laser beam was at $\lambda = 800$ nm, pulse width 65 fs, pulse repetition rate 1 kHz, and average power 3.5 W. 90% of the output beam was converted to 650 nm or 750 nm by use of optical parametric oscillator (Topas, Light Conversion) and were used for excitation (pump beam). The remaining 10% was used to generate white light continuum in CaF_2 plate (probe beam). The details on pump probe setup and measurement method are described in Ref. 17.

TPA coefficient was measured by open aperture Z-scan.[18,19] The input laser was from a tunable oscillator (MaiTai, Spectra-Physics, Inc.), with pulse width 100 fs, pulse repetition rate 80 MHz, tuning range from 710 to 920 nm. The beam radius at the focal point is calculated to be 16 μm. The femtosecond laser is focused by a 10 cm focal length lens. The sample was mounted on a computer controlled stage. The second lens was placed before the detector to collect all the transmitted light.

B. Theoretical methods

For all computations done in this work, quantum chemical program GAUSSIAN[20] was used. Ground state geometry of rubrene was optimized in vacuum using B3LYP DFT functional with 6-31G(d,p)[21–23] basis set. Computation of transition energies and transition dipole moments for the first 20 singlet vertical excited states of rubrene was carried out using time-dependent density functional theory method employing BH&HLYP[24,25] DFT functional and TZVP[26] basis set.

III. RESULTS AND DISCUSSION

A. Two-photon-induced transient absorption spectroscopy

In order to study the two-photon excited state relaxation process in rubrene single crystal, we applied the femtosecond pump probe technique under two-photon excitation. The pump wavelength is chosen at 650 nm, i.e., no linear absorption. Figure 1(b) shows the two-photon-induced TA spectra in rubrene. We measured the absorbance change (ΔA) in the TA measurements. The $\Delta A > 0$ indicates for the photo-induced absorption, while $\Delta A < 0$ indicates for the ground state bleaching or stimulated emission. Due to the group velocity dispersion (GVD) in the optical elements including the CaF_2 plate, the white light continuum probe is temporally chirped. We used the ultrafast nondegenerate two-photon absorption signal (*vide infra*) to do the chirp correction.[14]

In our previous work,[7] we have studied one-photon-induced singlet fission in rubrene single crystal by femtosecond pump-probe spectroscopy under 500 and 250 nm excitation. We have extended this approach to two-photon absorption induced singlet fission. From Fig. 1(b), the two-photon-induced transient absorption spectra after 3 ps show similar behaviour as one-photon TA spectra (from Ref. 7). Triplet-triplet absorption at 510 nm is still dominant in the two-photon-induced TA spectra, however, the decay of the excited singlet states S_1 is not as pronounced as one-photon absorption (OPA) TA spectra. Moreover, under two-photon excitation, the isosbestic point at 455 nm in OPA TA spectra[7] disappears. This is indicative that triplet states form not simply after the decay of excited singlet state S_1, however, there is also another channel for triplet states population. In the whole TA spectra, there are always two troughs located at 465 and 495 nm, which correspond well with the peak positions of steady state absorption spectrum (Fig. 1(a)). It is due to the overlap of negative ground state bleaching and the positive TA signal. The transient signal at negative time delays is indicative for long-lived transient states. The pulse repetition rate of our laser system is 1 kHz, i.e., the negative time delay is equivalent to 1 ms decay time. The ground state bleaching at negative times in Fig. 1(b) is due to the long-lived triplet states (about 0.2 ms, Ref. 7) formed via singlet fission.

In Fig. 1(b), there is a significant difference for the transient spectra between the early ($t < 0.5$ ps) and longer times ($t > 3$ ps). Moreover, the kinetics at different probe wavelengths (Fig. 2) show a fast process within first hundreds femtoseconds, and followed by a slower process at longer times. In femtosecond transient absorption spectroscopy, when the pump and probe beams spatially and temporally overlap, transient absorption spectra are sometimes distorted by the signal from "coherent artifact." The coherent artifact including two-photon absorption, stimulated Raman amplification, and cross-phase modulation,[27–29] is caused by the third order nonlinear susceptibility $\chi^{(3)}$. Figure 1(b) shows that the ultrafast

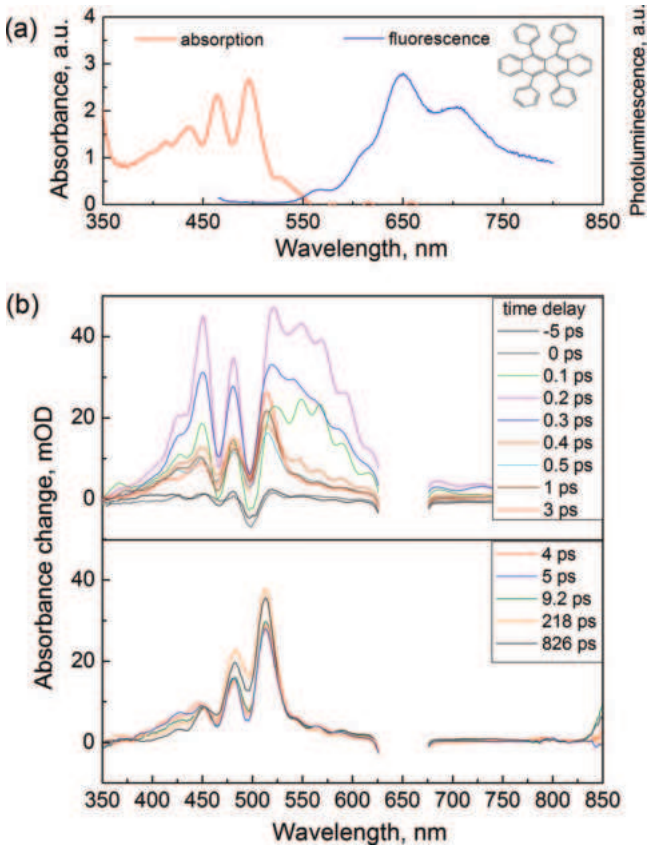

FIG. 1. (a) Steady state absorption and fluorescence spectra of rubrene single crystal (inset: molecular structure). (b) TA spectra for rubrene single crystal after chirp correction, $\lambda_{exc} = 650$ nm. The region 625–675 nm of strong scattered excitation light is removed. The upper and lower parts show the TA spectra at different time ranges.

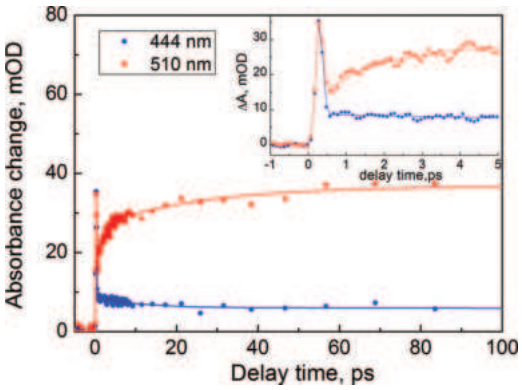

FIG. 2. Transient kinetics at 444 nm and 510 nm probe wavelengths. Inset shows the kinetics within the first 5 ps.

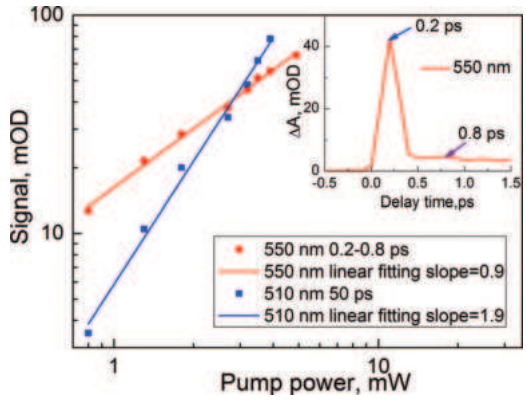

FIG. 3. Log-log plot of TA signal at different delay times (0.2 and 50 ps) of rubrene crystal as a function of pumping power, $\lambda_{exc} = 650$ nm. The inset shows the schematic of temporal positions at 550 nm probe chosen for the fast process.

transient absorption spectra in the first hundreds of fs are very broad, cover almost all the probe wavelengths range.

The fast (<500 fs) and slow (>500 fs) transient absorption signals are induced by the nondegenerate and degenerate two-photon absorption (D-TPA), respectively, based on the power dependence study. The power dependence of 510 nm transient signal (absorption peak of the slow process) at 50 ps and of 550 nm (large absorption for the fast process with low influence from slow process) at 0.2 ps are shown in Fig. 3. The transient signal of 550 nm at 0.8 ps (when the fast process is ended) is subtracted from the signal measured at 0.2 ps in order to get the contribution from fast process (see the inset of Fig. 3). Both the transient signal and pump power are shown on the log-log scale. The slopes are indicative of the order of the corresponding nonlinear process. For the ultrafast process, the slope is 0.9, i.e., linear dependence on the pump intensity. Since there is no linear absorption at 650 nm, the ultrafast process is induced by the ND-TPA process, i.e., one pump and one probe photon are simultaneously absorbed by the sample, and excite the molecules to two-photon excited state.[15,30] As for the slow process, the slope of the linear fit is 1.9, indicative for the quadratic dependence on the pump intensity. Therefore, the slow process is generated by D-TPA process, i.e., absorption of two photons with the same photon energy. The transitions for the ND- and D-TPA are shown in Fig. 4(a).

Rubrene molecule is centrosymmetric, the selection rules for OPA and TPA transitions are different. For instance, for one-photon transition, a change of parity is required. However, two-photon transitions must have the same symmetry for the initial and final states.[12,13] In order to obtain the location of the TPA excited states, the ND-TPA spectrum was studied in detail. First, Negres *et al.*[30] have used pump probe technique in order to get the ND-TPA spectrum. The ND-TPA spectra obtained by pump-probe show good agreement with the D-TPA studied by other methods, e.g., Z-scan[31] and two-photon fluorescence spectroscopy.[30] The ultrafast TA spectrum induced by the ND-TPA process under 650 nm pump wavelength covers the whole probe range of 350-850 nm (Fig. 1(b)).

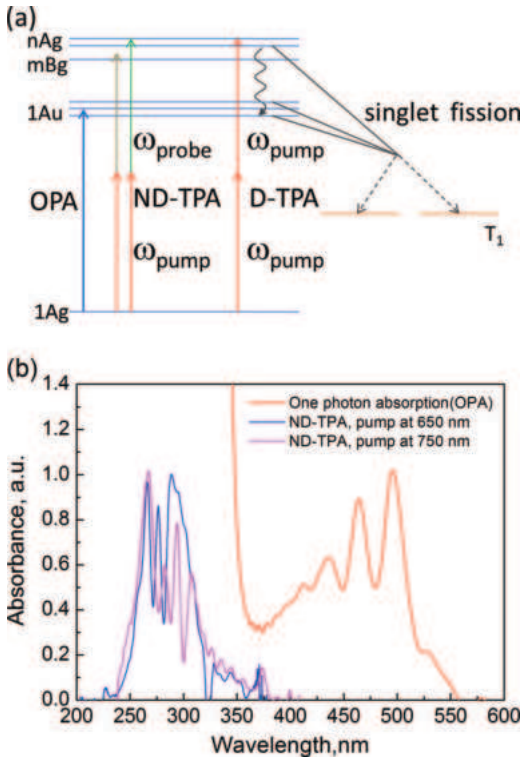

FIG. 4. (a) Schematic of the transitions for one-photon absorption (OPA), nondegenerate two-photon absorption (ND-TPA), and degenerate two-photon absorption (D-TPA) processes. (b) OPA and ND-TPA spectra (under 650 and 750 nm pump).

In order to get the ND-TPA spectrum, the TPA wavelength (λ_{TPA}) was calculated according to the equation

$$\frac{1}{\lambda_{TPA}} = \frac{1}{\lambda_{pump}} + \frac{1}{\lambda_{probe}}, \quad (1)$$

where λ_{pump} and λ_{probe} are the pump and probe wavelengths, respectively. The obtained ND-TPA spectra under 650 and 750 nm pump wavelengths together with the linear (one-photon) absorption spectrum are plotted in Fig. 4(b). The two ND-TPA spectra correspond very well, only the valleys features are shifted. The valley structures are caused by the ground state bleaching in the TA spectra, which is determined by the linear absorption spectrum. Therefore, the ground state bleaching positions are the same in the measured TA spectra under different λ_{pump}. But after conversion to λ_{TPA} according to Eq. (1), the positions of these valley structures will be shifted due to different λ_{pump}. Comparing the OPA and ND-TPA spectra (Fig. 4(b)), we can conclude that the two-photon excited states are located well above the one-photon excited states.

The transient kinetics at 444 nm ($S_1 \rightarrow S_N$ peak) and 510 nm ($T_1 \rightarrow T_N$ peak) are shown in Fig. 2. In order to fit the ultrafast ND-TPA process, one ultrafast time component $\tau_0 \leq 150$ fs is needed for all transient kinetics. Apart from the fast femtosecond ND-TPA, transient signal at 444 nm decays with two components: $\tau_1 = 11$ ps ($A_1 = 31\%$) and $\tau_2 > 2$ ns ($A_2 = 69\%$). TA signal at 510 nm develops with two rise components $\tau_1 = 1.6$ ps ($A_1 = 56\%$), $\tau_2 = 23$ ps ($A_2 = 44\%$) due to the singlet fission, and does not show decay in 1 ns time

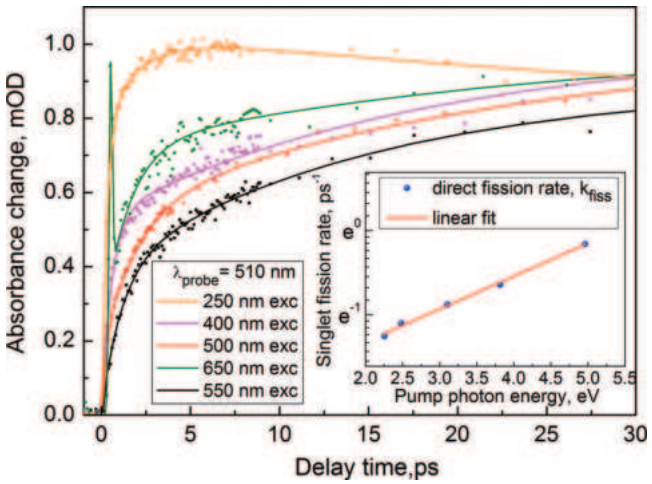

FIG. 5. Normalized transient absorption kinetics at $\lambda_{probe} = 510$ nm under OPA (250–550 nm) and TPA (650 nm). (Inset) Arrhenius plot of singlet fission rate versus pump photon energy.

window. TA signal of S_1 overlaps with TA of T_1. Therefore, decay of 444 nm peak includes a long time component ($\tau_2 > 2$ ns), which is due to triplet state decay. The fast component of S_1 decay (11 ps) is due to thermally activated fission from the lowest vibrational level of S_1. Comparison of the triplets rise time under different excitation wavelengths is shown in Fig. 5. All transient kinetics are at probe wavelength $\lambda = 510$ nm and normalized at their maxima: the kinetics under 400–650 nm excitation were normalized at 400 ps; while the kinetics under 250 nm was normalized at 6.3 ps. From Fig. 5, we can see that the rise time of triplet states, i.e., singlet fission rate, is pump wavelength dependent. In the OPA region (250–550 nm), the triplet states form faster with decreasing pump wavelengths (i.e., increasing pump photon energy). It points out singlet fission can proceed directly from various excited states, i.e., higher excited singlet states S_N (under 250 nm), or upper vibrational states of S_1 (400–550 nm). The energy of the lowest excited singlet state $E(S_1) = 2.23$ eV (determined from the absorption spectrum), and the energy of the triplet state is $E(T_1) = 1.14$ eV,[32] therefore, the energy difference $E(S_1) - 2E(T_1) = -0.05$ eV. Singlet fission is faster from the upper excited states since it is exoergic; however, it becomes slower from the lowest excited state S_1 since it is endoergic. Under different pump wavelengths, there are always two rise-time constants for the formation of triplet states: $\tau_1 \sim 2$ ps and $\tau_2 \sim 20$ ps. We assign the faster τ_1 to the direct singlet fission from the upper excited singlet states S_N or upper vibrational levels of S_1, and the longer $\tau_2 \sim 20$ ps to the thermally activated fission from the lowest vibrational levels of S_1. Therefore, τ_1 will vary while τ_2 is invariant with the excitation wavelength. For all the kinetic curves in Fig. 5, global fit was performed by use of free τ_1 and fixed τ_2. The global fit results in $\tau_2 = 34$ ps, τ_1 ranges from 1.2 to 3.5 ps under different excitation wavelengths (250–650 nm), shown in Table I. Another longer time constant $\tau_3 > 1$ ns is needed to fit the long lived decay of triplet ($\lambda_{pump} = 400$–650 nm) or polaron ($\lambda_{pump} = 250$ nm). The direct singlet fission from TPA excited states is faster than the fission from S_1 state, and slower

TABLE I. Global fit results for 510 nm transient kinetics under different pump wavelength (λ_{pump}).

λ_{pump} (nm)	τ_1 (ps)	A_1[a]	τ_2 (ps)	A_2[a]	τ_3 (ps)	A_3[a]
250	1.2	−0.50	34	−0.27	1400	1.0
650[b]	1.9	−0.36	34	−0.26	10 000	1.0
400	2.4	−0.27	34	−0.36	10 000	1.0
500	3.0	−0.42	34	−0.35	10 000	1.0
550	3.5	−0.32	34	−0.43	10 000	1.0

[a] A_1, A_2, and A_3 are the fractional amplitudes of different time constants. $A > 0$: decay process; $A < 0$: rise process.
[b] Under 650 nm two-photon excitation.

than from S_N states. It means that two-photon excited states are located between S_1 and S_N. The relation between the direct singlet fission rate $k_{fiss} = 1/\tau_1$ versus the pump photon energy is shown in the inset of Fig. 5. The $\ln(k_{fiss})$ undergoes a linear increase with excitation photon energy, i.e., follows the Arrhenius law:

$$k_{fiss} = A \exp\left(-\frac{E_a}{RT}\right), \quad (2)$$

where A is the pre-exponential factor, R is the molar gas constant, T is temperature, and E_a is the activation energy, i.e., $E_a = 2E(T) - E_{exc}$ (E_{exc} is the excitation energy).

Based on all the discussion above, we can conclude that singlet fission can proceed in picosecond time scale directly from the upper excited states S_N, upper vibrational states of S_1, or two-photon excited states bypassing S_1 state. The relaxation process of rubrene single crystal under two-photon excitation is shown in Fig. 4(a): direct singlet fission takes place within 1.6 ps, and it competes with the fast internal conversion. 40% of the two-photon excited states relax to the lowest one-photon excited state S_1, where triplet states continue to be formed, even though 15 times slower via thermally activated fission.

Tao *et al.*[5] also studied the relaxation dynamics of photoexcited excitons in rubrene crystal by use of femtosecond pump-probe technique. They explain the decay of excitons being due to the dissociation to polarons. However, in our previous article,[7] we have clearly demonstrated that the formation of polarons is an ultrafast process ($\ll 100$ fs). The decay of singlet excitons equals to the rise time of the triplets. Therefore, the singlet fission is the main channel of exciton relaxation. It should be noted that in Ref. 5, the triplet state transient was not monitored.

B. Two-photon absorption coefficient

The TPA coefficient of rubrene crystal was measured by open aperture Z-scan method under femtosecond laser excitation: 740 nm, i.e., no linear absorption (Fig. 1(a)). The calculated TPA coefficient is 52 cm/GW (Fig. S1(a) in the supplementary material[33]). In order to figure out whether the singlet fission influences the TPA coefficient, TPA is also studied in rubrene solution (toluene) where singlet fission is absent.[7] The TPA cross section of rubrene solution is $\sigma = 540$ GM (1 GM $= 10^{-50}$ cm^4 s photon^{-1}). By estimating the "concentration" (number of molecules per unit volume) of

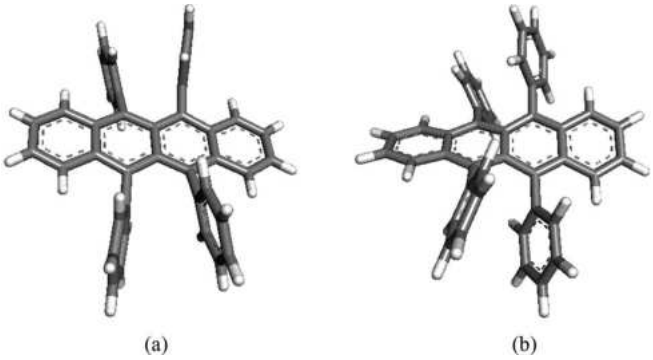

FIG. 6. Rubrene molecule conformations in single crystal (a) and solution (b).

molecules in rubrene crystal, the TPA cross section for crystal can also be determined; $\sigma = 1000$ GM. It is the same order of magnitude with solution case. Therefore, we can conclude that the singlet fission (participation of the triplet states) does not influence the two-photon absorption process.

C. Quantum chemical calculations

Two-photon allowed transitions have been selected among computed singlet excited states in accord with the selection rules. It is noteworthy, that the geometry of rubrene differs dependent on the phase and state. Thus in single crystal, the molecules of rubrene have C_{2h} (2/m) symmetry[34,35] with a nearly planar tetracene backbone (Fig. 6(a)); in solution and amorphous phase, rubrene shows D_2 (222) symmetry,[36–38] characterized by a twisted tetracene backbone (Fig. 6(b)). As it was already pointed out in Ref. 28, the optimized ground state structure of rubrene in vacuum corresponding to the C_{2h} symmetry is a first-order saddle point and, that it is stabilized in crystal owing to the crystal-packing forces. Our computation revealed that the backbone of C_{2h}-rubrene is not quite planar. Eight of its carbons are located 8° or 2° out of plane made by the other ten carbons of the backbone as shown in Fig. S3 in the supplementary material.[33] Optimized geometry of C_{2h}-rubrene in Cartesian coordinates is available in the supplementary material.[33] Results of our computations for vertical singlet excited states of C_{2h}-rubrene are summarized in the Table S1 in the supplementary material.[33] According to the selection rules for molecules owning an inversion center, transitions are allowed between electronic states with opposite parity only, in case of one-photon absorption; and between electronic states with the same parity only, in case of two-photon absorption. Hence, one- and two-photon allowed transitions are mutually exclusive and clearly distinguishable for C_{2h}-rubrene.

The dominant dipole-allowed transition in the visible region appearing at 490 nm (Table S1 in the supplementary material[33]) is due to migration of an electron from the donor HOMO to the acceptor LUMO molecular orbital, which is accompanied by change of the parity from even to odd for the initial A_g and the final A_u electronic states, respectively. This agrees well with our steady state one-photon absorption spectrum.[7] Deviation of 6 nm from the measured wavelength may be caused by the basis set of only moderate quality used in this work. In our preliminary tests, we revealed improvement of 13 nm between results obtained when basis sets of double-ζ or triple-ζ quality were used.

Transitions in TPA spectrum of C_{2h}-rubrene, will have even parity in line with ground electronic state A_g. Among all theoretical excited states with even parity (Table S1 in the supplementary material[33]), the one with lowest transition energy is at 313 nm ($A_g \rightarrow B_g$, 34% H-3→LUMO, 56% H-2→LUMO, and 7% HOMO→L+2), well separated from the dipole allowed one-photon transition (HOMO→LUMO). It confirms our conclusion that the two-photon excited states are located well above the one-photon excited states. Compared with our experimental ND-TPA spectrum (Fig. 4(b)), the computed $A_g \rightarrow A_g$ transition at 278 nm, corresponding to the promotion of an electron from HOMO to LUMO+3 molecular orbital (Table S1 in the supplementary material[33]), is the most favourable two-photon allowed transition. The electronic levels of rubrene are illustrated in Fig. 4(a), where the ground state is labelled with $1A_g$, the lowest one-photon excited state with $1A_u$, and two-photon excited states with mB_g and nA_g. The one- and two-photon absorption properties of rubrene were also calculated by Zhao *et al.*[12] by adopting the INDO/SDCI (intermediate neglect of differential overlap including configuration interaction with single and double excitations) method. However, they chose the D_{2h} (mmm) conformation which is neither crystal nor solution geometry.

IV. CONCLUSIONS

Two-photon-induced singlet fission in rubrene single crystal was observed for the first time by femtosecond pump-probe spectroscopy. Dynamics of the two-photon excited state relaxation was analysed. Direct singlet fission takes place from the two-photon excited states, competed with the internal conversion to the lowest excited singlet state S_1. Non-degenerate two-photon absorption spectrum was attained from the two-photon-induced transient absorption spectra. Two-photon absorption coefficients of rubrene single crystal and solution were determined by Z-scan method; TPA cross sections were shown to be similar, which indicates that there is no contribution of singlet fission to TPA. Quantum chemical calculations support the TPA experimental data.

ACKNOWLEDGMENTS

We thank Dr. Tingchao He for the help with Z-scan and two-photon PL measurements. We would also like to acknowledge IT Team at the School of Physical and Mathematical Sciences for provided computational time.

[1] V. Podzorov, E. Menard, A. Borissov, V. Kiryukhin, J. A. Rogers, and M. E. Gershenson, Phys. Rev. Lett. **93**, 086602 (2004).
[2] V. C. Sundar, J. Zaumseil, V. Podzorov, E. Menard, R. L. Willett, T. Someya, M. E. Gershenson, and J. A. Rogers, Science **303**, 1644 (2004).
[3] A. Saeki, S. Seki, T. Takenobu, Y. Iwasa, and S. Tagawa, Adv. Mater. **20**, 920 (2008).
[4] A. Yildiz, P. T. Kissinger, and C. N. Reilley, J. Chem. Phys. **49**, 1403 (1968).
[5] S. Tao, H. Matsuzaki, H. Uemura, H. Yada, T. Uemura, J. Takeya, T. Hasegawa, and H. Okamoto, Phys. Rev. B **83**, 075204 (2011).

[6]A. Furube, R. Katoh, H. Mitsuta, T. Miyadera, and Y. Yoshida, ECS Meet. Abstr. **1101**, 1831 (2011).
[7]L. Ma, K. Zhang, C. Kloc, H. Sun, M. E. Michel-Beyerle, and G. G. Gurzadyan, Phys. Chem. Chem. Phys. **14**, 8307 (2012).
[8]A. Ryasnyanskiy and I. Biaggio, Phys. Rev. B **84**, 193203 (2011).
[9]B. A. West, J. M. Womick, L. E. McNeil, K. J. Tan, and A. M. Moran, J. Phys. Chem. C **114**, 10580 (2010).
[10]C. E. Swenberg and N. E. Geacintov, *Organic Molecular Photophysics* (Wiley & Sons Ltd., Chichester, Sussex, 1973), Vol. 18.
[11]M. Pope and C. E. Swenberg, *Electronic Processes in Organic Crystals and Polymers*, 2nd ed. (Oxford University Press, Oxford, UK, 1999).
[12]L. Zhao, G. Yang, Z. Su, C. Qin, and S. Yang, Synth. Met. **156**, 1218 (2006).
[13]K. S. Bindra, C. P. Singh, S. M. Oak, R. Sailaja, and P. B. Bisht, Opt. Laser Technol. **43**, 1486 (2011).
[14]R. A. Negres, J. M. Hales, A. Kobyakov, D. J. Hagan, and E. W. Van Stryland, IEEE J. Quantum Electron. **38**, 1205 (2002).
[15]X. Zhang, Y. Xia, R. H. Friend, and C. Silva, Phys. Rev. B **73**, 245201 (2006).
[16]C. Kloc, P. G. Simpkins, T. Siegrist, and R. A. Laudise, J. Cryst. Growth **182**, 416 (1997).
[17]J. Shang, T. Yu, J. Lin, and G. G. Gurzadyan, ACS Nano **5**, 3278 (2011).
[18]M. Sheik-Bahae, A. A. Said, T. H. Wei, D. J. Hagan, and E. W. Van Stryland, IEEE J. Quantum Electron. **26**, 760 (1990).
[19]T. He, W. Wei, L. Ma, R. Chen, S. Wu, H. Zhang, Y. Yang, J. Ma, L. Huang, G. G. Gurzadyan, and H. Sun, Small **8**, 2163 (2012).
[20]M. J. Frisch, G. W. Trucks, H. B. Schlegel *et al.*, GAUSSIAN 09, Revision B.01, Gaussian, Inc., Wallingford, CT, 2010.
[21]W. J. Hehre, R. Ditchfield, and J. A. Pople, J. Chem. Phys. **56**, 2257 (1972).
[22]P. C. Hariharan and J. A. Pople, Theor. Chim. Acta **28**, 213 (1973).
[23]M. M. Francl, W. J. Pietro, W. J. Hehre, J. S. Binkley, M. S. Gordon, D. J. DeFrees, and J. A. Pople, J. Chem. Phys. **77**, 3654 (1982).
[24]C. Lee, W. Yang, and R. G. Parr, Phys. Rev. B **37**, 785 (1988).
[25]A. D. Becke, J. Chem. Phys. **98**, 1372 (1993).
[26]A. Schafer, C. Huber, and R. Ahlrichs, J. Chem. Phys. **100**, 5829 (1994).
[27]K. Ekvall, P. v. d. Meulen, C. Dhollande, L.-E. Berg, S. Pommeret, R. Naskrecki, and J.-C. Mialocq, J. Appl. Phys. **87**, 2340 (2000).
[28]M. Lorenc, M. Ziolek, R. Naskrecki, J. Karolczak, J. Kubicki, and A. Maciejewski, Appl. Phys. B **74**, 19 (2002).
[29]B. Dietzek, T. Pascher, V. Sundström, and A. Yartsev, Laser Phys. Lett. **4**, 38 (2007).
[30]R. A. Negres, J. M. Hales, A. Kobyakov, D. J. Hagan, and E. W. Van Stryland, Opt. Lett. **27**, 270 (2002).
[31]H. Hu, D. A. Fishman, A. O. Gerasov, O. V. Przhonska, S. Webster, L. A. Padilha, D. Peceli, M. Shandura, Y. P. Kovtun, A. D. Kachkovski, I. H. Nayyar, A. E. Masunov, P. Tongwa, T. V. Timofeeva, D. J. Hagan, and E. W. Van Stryland, J. Phys. Chem. Lett. **3**, 1222 (2012).
[32]W. G. Herkstroeter and P. B. Merkel, J. Photochem. **16**, 331 (1981).
[33]See supplementary material at http://dx.doi.org/10.1063/1.4804398 for the two-photon absorption cross section and quantum chemical calculation results.
[34]O. D. Jurchescu, A. Meetsma, and T. T. M. Palstra, Acta Crystallogr., Sect. B: Struct. Sci. **62**, 330 (2006).
[35]A. S. Paraskar, A. R. Reddy, A. Patra, Y. H. Wijsboom, O. Gidron, L. J. W. Shimon, G. Leitus, and M. Bendikov, Chem. Eur. J. **14**, 10639 (2008).
[36]T. Petrenko, O. Krylova, F. Neese, and M. Sokolowski, New J. Phys. **11**, 015001 (2009).
[37]D. Käfer, L. Ruppel, G. Witte, and C. Wöll, Phys. Rev. Lett. **95**, 166602 (2005).
[38]M. Kytka, L. Gisslen, A. Gerlach, U. Heinemeyer, J. Kovac, R. Scholz, and F. Schreiber, J. Chem. Phys. **130**, 214507 (2009).